Diffusion and magnetic relaxation in model porous media

Aniket Bhattacharya and S. D. Mahanti
Department of Physics, Michigan State University and Center for Fundamental Material Research, East Lansing, Michigan 48824-1116

Amitabha Chakrabarti
Department of Physics, Kansas State University, Manhattan, Kansas 66506-2601
(Received 24 August 1995; revised manuscript received 21 November 1995)

Diffusion and magnetic relaxation are studied in computer-generated model two-dimensional porous media whose three-dimensional analogs resemble commercially prepared Vycors and aerogels. When diffusion rates are compared for two different samples, one with average pore diameter much shorter than the other but with the same porosity, a *crossover* is observed where the asymptotic long-time diffusion rate $D(t)$ for the smaller pore becomes larger than the bigger one. However, this *crossover* disappears for relatively larger pores of fixed porosity. Physically, this crossover is a characteristic of changed surface morphology where for a fixed porosity, pore diameters could be made bigger but at the cost of separating the pores from each other by thin but more ordered walls, linked to each other with very narrow necks. This results in a net decrease in the long-time diffusion constant. We have also been able to relate this *crossover* to the absence of *dynamical scaling* for the structures. Adding a surface relaxation term at the pore walls *increases* the effective diffusion rate at early times. We compare our simulation results for the model systems, wherever possible, with some of the general results for porous media obtained analytically.

I. INTRODUCTION

Understanding various physical processes such as fluid transport, phase transitions, etc., occurring inside porous media and how they are influenced by the geometry and disorder has attracted a great deal of both experimental and theoretical attention for the last several decades. Examples of porous media are naturally occurring rocks, biological cells, zeolites, intercalated layered systems such as pillared lamellar oxides and more recently discovered nano and meso tubes like MCM-41. Measurement of magnetic relaxation and diffusivity has been routinely used to extract information about the geometry and connectivity of these porous media. Many of the earlier work on porous media have dealt with models of highly consolidated structures of naturally occurring sandstones and rocks[1] and commercially synthesized zeolites whose porosities can be extremely low. In this paper we have explored diffusion and magnetic relaxation in a class of two-dimensional model porous media of relatively larger porosities with varying degree of nonuniformity and connectivity. One of the key features of these computer-generated model porous media is that for a fixed porosity it is possible to generate structures with very different surface morphologies. These structures have very marked effect on both the short- and long-time diffusion rates. Furthermore these morphologies can be changed in a controlled manner which enables us to study transport and relaxation in a very systematic way.

Nuclear magnetic relaxation has been widely used to extract information about transport processes in porous media in general and the fluid-saturated porous media in particular. In a proton NMR experiment in the latter system, the rate of decay of magnetization depends on the characteristic length scales of the pore space and on the interactions at the pore grain interface. The additional interaction of protons with paramagnetic impurities located on the grain surface enhances the relaxation process. The continuum description of this process has traditionally been described through diffusion equation. The effect of the surface relaxers are taken into account through boundary condition at the pore surface. In one of the pioneering works in this field Brownstein and Tarr[2] made a very important observation that for very small pores the decay was multiexponential, the geometry of the pore being the decisive factor for the relevant time scales for the magnetic relaxation. Since then a number of approaches have been developed to study particle diffusion in such restricted geometries in general. The method of random walkers[3,4] has proven to be a very successful tool. It has been widely used to extract information about permeability in several models of rocks.[3] More recently in a series of papers Sen and co-workers,[5,6] and Mitra and Sen[7,8] have extensively analyzed the diffusion and relaxation processes in porous media starting from the diffusion equation. They have derived analytic results for periodic geometries to illustrate the important differences between diffusion rates for the cases when the surface relaxivity $\rho=0$ and $\rho\neq 0$. Bergman and Dunn[9] have developed a method of matrix eigenvalue problem for the diffusion eigenstates of a periodic porous media. The later approach seems to be complementary to the method of Mitra *et al.*, and in many of the cases they give identical results.[10]

In this paper we have ventured away from the well-studied cases of porous rocks or periodic geometries; our focus is on two different types of porous media, which resemble Vycor and aerogel. The porosity of these media are significantly higher. Secondly these are examples of correlated disorder where in addition to porosity, the surface morphology plays a very crucial role. The motivation for this work also comes from various other recent theoretical and experimental studies on Vycor and aerogels; it has been observed that these porous media have dramatic effects on the

phase transition and dynamics of confined fluids.[11]

Another aspect of these computer-generated porous media is that they are highly controllable and therefore it is possible to make a systematic study of diffusion and magnetic relaxation processes. For simplicity we consider two-dimensional (2D) models in this paper. However many of our results are quite general and should be applicable to the more realistic 3D systems. In the following section we describe in detail the underlying theory of preparation of model Vycors and aerogels. In the next two sections we give a brief history of earlier work, present our results on the time dependence of diffusion rates and spatially averaged magnetic moment, and compare our work with the earlier ones, wherever possible. The last section gives a summary and then describes the work in progress.

II. METHOD

A. Preparation of model 2D Vycor

Vycor is a porous glass. In reality these are prepared from the phase-separated borosilicate glass by acid etching of the boron.[12] The underlying theory to produce a computer-generated Vycor is the dynamics of a first-order phase separation process for a binary mixture. It is now well known that a binary mixture when quenched deep inside the coexistence regime undergoes a phase separation process driven by small amplitude large wavelength fluctuations of the order parameter, known as spinodal decomposition. The two components form an interconnected structure. At late times a single time-dependent length scale $R(t)$ associated with the domain sizes of the two components govern the physics which implies that the correlation function $C(\mathbf{r},t)$ of the order parameter $\phi(\mathbf{r},t)$, defined as

$$C(\mathbf{r},t)=L^{-d}\int d^d r' \langle \phi(\mathbf{r}+\mathbf{r}',t)\phi(\mathbf{r},t)\rangle, \tag{1}$$

obeys a simple *dynamical scaling* law

$$C(\mathbf{r},t)=g(r/R(t)), \tag{2}$$

where d is the spatial dimensionality of the system. Alternatively, its Fourier transform, the structure factor $S(\mathbf{k},t)=\langle \phi_{\mathbf{k}}(t)\phi_{-\mathbf{k}}(t)\rangle$ exhibits the following scaling form:

$$S(\mathbf{k},t)=R^d(t)s(kR(t)). \tag{3}$$

The details of the kinetics of first-order phase transition could be found in many excellent review articles listed in Refs. 13 and 14. The dynamics is usually described by a coarse-grained Cahn-Hilliard-Cook equation,[13] which belongs to the same universality class as the spin-exchange Kawasaki dynamics for the kinetic Ising model.[15] An alternate approach for the coarse-grained description is due to Oono and Puri[16] which is usually known as the *cell dynamics* method. In this work we have used the cell dynamics method to prepare the computer-generated 2D Vycors. Although, some characteristics of these numerically generated structures are quite different from commercially available Vycor glass,[12] we will loosely call these interconnected structures Vycors in this paper.

The Cahn-Hilliard or cell dynamics approach is a field-theoretic description so that the concentration field $\psi(\mathbf{r},t)$ describing the mixture (order parameter) takes continuous values anywhere from -1 to $+1$. Starting from an initial zero value of the order parameter (i.e., a 50:50 mixture of the two components, or $\langle \psi(\mathbf{r},0)\rangle=0$) as the coarsening time (t_{coarse}) increases the separation process drives the field variables toward either $+1$ or -1. Although the linear size of domains of each component grows with time, the porosity always remains close to 50% since the order parameter is *conserved*. However one can define a *cutoff* value for the order parameter ψ_{etch} such that order-parameter values for which $\psi \leqslant \psi_{\text{etch}}$ will consist of the pore space and the values for which $\psi > \psi_{\text{etch}}$ will be interpreted as glass. We call this procedure *etching* in this paper.[17] By adjusting the cutoff value for the order-parameter ψ_{etch} the porosity may be varied over a wider range. To make this point more explicit we have shown an example in Fig. 1. Figures 1(a) and 1(b) show a phase separated mixture at $t_{\text{coarse}}=100$ and 1000 (in arbitrary unit). The corresponding cutoff values (ψ_{etch}) are 0.49 and 0.885 (i.e., from -1 up to 0.49 or up to 0.885 is the pore space, the rest is glass) which produce Vycors of 80% porosity with average diameters 10.8 and 17.8, respectively. We have used the coarsening time t_{coarse} and the etching value for the field ψ_{etch} as two tunable parameters to prepare model Vycors of different porosities and average pore diameters. The surface to volume ratio (S/V), which is a key geometrical parameter is then obtained from the coordinates of the pore and glass space. Similarly Figs. 1(c) and 1(d) refers to two different aerogel samples of 80% porosity and average pore diameter 9.1 and 13.4, respectively, prepared by varying the aggregation time (see below).

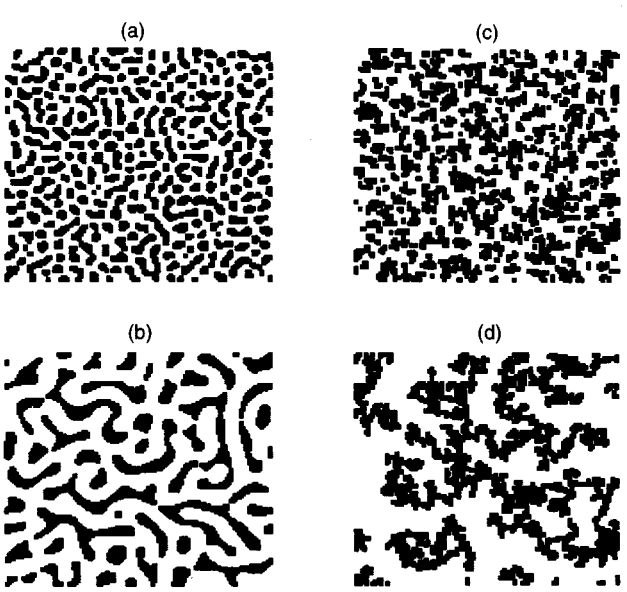

FIG. 1. Pictures of computer-generated 2D model Vycors and aerogels of 80% porosity. (a) and (b) correspond to model Vycors with average pore diameters 10.8 and 17.8, respectively. (c) and (d) correspond to model aerogels with average pore diameters 9.1 and 13.35, respectively.

B. Preparation of model 2D aerogel

The model aerogel is prepared by diffusion limited cluster aggregation (DLCA) method.[18] Initially each cluster consists

of a single particle. For a given porosity the number of particles is fixed (for a fixed size lattice). As time proceeds they aggregate irreversibly to form bigger clusters. The clusters also diffuse rigidly and stick irreversibly when they come into contact with other clusters. In three dimensions, this model is a good representation of an aerogel structure.[18] It is also known that the structures generated this way show dynamical scaling behavior similar to spinodally decomposed binary mixtures at late times.[19] The average pore radius and the surface-to-volume ratio is then controlled by monitoring the aggregation time. We will again loosely call these two-dimensional structures aerogels. For a set of aerogels (or model Vycors) with fixed porosity, bigger pore radii would reflect surfaces with bigger correlation length. Therefore the diffusion rate measured in this set will provide information about how the surface morphology affects the diffusivity in this medium.

C. Random-walk method

Random walkers have been used earlier to study transport and magnetic relaxation in porous rocks.[3,4] It is also possible to model pulsed gradient NMR by a random walker by attributing additional phases proportional to the local magnetic field to each walker.[4] After generating a model porous system we have checked if the pore space percolates and then let random walkers move around one at a time starting from different initial positions inside the pore space. For any attempted move by the walker towards a grain boundary it stays at the same point but the clock advances one unit. For magnetic relaxation studies the proton magnetization of the walker decays at the grain boundary with a probability γ. Obviously γ and the surface-relaxation strength ρ appearing in boundary conditions for the diffusion equation[2] are interrelated. For very weak relaxation it can be shown that $\rho=\gamma/(1-\gamma)$.[1] But in general there is no well-defined formula to convert one from the other.[9,20] In this work we will describe our results in terms of $\gamma=1-p_f$ (p_f is the survival probability) and use ρ and γ synonymously.

For each sample the initial position of the walker is averaged over 500 different locations inside the pore space. The final average is done with results for 200 samples. We have checked that statistical uncertainties in the results obtained after this large sample averaging is extremely small. For a fixed set of parameters the results for two independent sets are hardly distinguishable. In all the results shown here the Vycor is embedded on a 128×128 square lattice. We have checked by taking a few runs on 256×256 lattice that the results are hardly distinguishable. Therefore we have taken most of our runs on 128×128 lattices. This enabled us to perform many sample averages which is extremely crucial to reduce statistical fluctuations associated with disordered systems.

III. EARLIER WORK

The effects of the surface magnetic impurities on the magnetic relaxation were studied by Brownstein and Tarr[2] in the context of a single spherical cell. Magnetic relaxation in this case is multiexponential and the time dependence of average magnetization $M(t)$ is given by

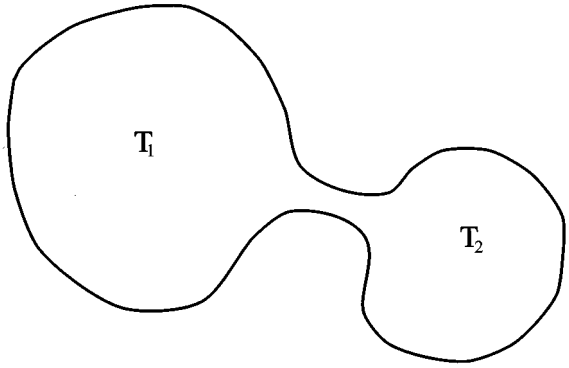

FIG. 2. Two pores connected by a narrow throat. Each pore relaxes with its characteristic relaxation time.

$$M(t)=\sum_{n=1}^{\infty} A_n \exp\left(-\frac{t}{T_n}\right). \tag{4}$$

The complete set of eigenfunctions A_n and eigenfrequencies T_n are obtained from the solution of the diffusion equation

$$D_0\nabla^2 M-\frac{\partial M}{\partial t}=0, \tag{5}$$

where D_0 is the bulk diffusion constant and the effect of the surface relaxation is incorporated through the boundary condition

$$[D_0\hat{n}\cdot M+\rho M]_S=0. \tag{6}$$

In Eq. (3) ρ is the surface relaxation strength. The presence of the surface relaxation introduces another scale into the problem which is conveniently expressed in terms of a dimensionless parameter

$$\overline{\rho}=\frac{\rho a}{D_0}. \tag{7}$$

It governs the competition between how fast the diffusion takes place and how rapidly the walkers get killed at the surface and therefore characterizes the over all relaxation process. In two extreme limits the characteristic single relaxation times are

$$T_{\text{surface}}=\begin{cases}\dfrac{a^2}{D_0}, & \dfrac{\rho a}{D_0}\gg 1\\[2ex] \dfrac{a}{\rho}, & \dfrac{\rho a}{D_0}\ll 1.\end{cases} \tag{8}$$

In the fast diffusion regime ($\rho a/D_0\ll 1$) the magnetization becomes uniform over the entire pore volume very rapidly and the smallest relaxation time (denoted as T) governs the diffusion problem. On the other hand in the slow diffusion regime ($\rho a/D_0\gg 1$), it is basically the time a particle takes to diffuse to the surface (a^2/D_0) that governs the relaxation process.[21]

Now consider the case where, instead of one pore, two pores of different average radii are connected through a neck[23] as shown in Fig. 2. Assuming the fast diffusion condition holds and the link between the pores is weak the two

pores will then relax with their characteristic decay times It can be shown that in the case where many pores are joined by such weak links the decay is given by

$$M(t)\sim\int_0^\infty P\left(\frac{1}{T}\right)\exp\left(-\frac{t}{T}\right)d\left(\frac{1}{T}\right). \tag{9}$$

The decay is in general nonexponential. If the diffusion is not sufficiently fast then one has to include other modes on top of the lowest mode in each pore. Therefore we notice that for a general situation the presence of many relaxation times may arise not only from a single pore but from a distribution of pore sizes as well which makes it intrinsically very difficult to extract information about pore geometries from the decay of $M(t)$.

However recent analytic treatments of the diffusion problem starting from the diffusion equation[5–8] have made some general predictions about the diffusion coefficient and its effect on surface relaxation. Let us define the time-dependent diffusion rate $D(t)$ as $\langle r^2(t)\rangle_s/2dt$, where $\langle r^2(t)_s\rangle$ is the mean-square displacement for those walkers which have *survived* until time t and d is the spatial dimension. Then for very early time it is shown that

$$\frac{D(t)}{D_0}=1-\frac{4}{9\sqrt{\pi}}\frac{S}{V}\sqrt{D_0t}-\frac{S}{12V}\left\langle\frac{1}{R_1}+\frac{1}{R_2}\right\rangle D_0t + \frac{1}{6}\frac{\rho S}{V}D_0t+\cdots, \tag{10}$$

and the net magnetization decreases as

$$M(t)=1-\rho t\frac{S}{V}, \tag{11}$$

where S and V are the pore surface area and pore volume, R_1 and R_2 are the two principal radii of curvatures of the pore walls. The origin of the $\sqrt{t}$ term in Eq. (7) comes from the fact that molecules which are within $D_0\sqrt{t}$ distance away from the pore surface are the ones who get affected by the surface and contribute to a decrease in the value of the diffusion rate. It is interesting to note that the presence of the surface relaxers only affects in the order $(\sqrt{t})^2$.

The long-time diffusion constant in a porous media is usually written in the following way:[23,24]

$$\frac{D(t)}{D_0}=\frac{1}{\alpha_0}+\frac{\alpha_1}{t}+\frac{\alpha_2}{t^{3/2}}+\cdots, \tag{12}$$

where α_0 is known as tortuosity of the porous material which in addition to other variables depend on the porosity ϕ.

In the fast diffusion regime for periodic systems with nonoverlapping spherical grains it has been shown by Mitra and Sen[8] that the long-time diffusion constant is given by

$$\lim_{t\to\infty}\frac{D_{\rm eff}}{D_0}=\frac{2}{3-\phi}-\rho^*A(\phi), \tag{13}$$

where $A(\phi)$ is a function of the porosity only. It is to be noted that no other geometrical factor enters into this case. One can show from a simple scaling argument that Eq. (13) is true for regular periodic geometries. As an example let us consider Figs. 3(a) and 3(b), respectively, where the porous media consist of periodic arrays of squares. In each case the porosity is kept fixed at 0.75, but S/V has been reduced by half in Fig. 3(b) compared to Fig. 3(a). Under a simple scale transformation $x\to\alpha x$ and $t\to\alpha^2t$ the diffusion constant remains invariant since $D=\Delta x^2/\Delta t$. [When $\alpha=2$, Fig. 3(a) will result in Fig. 3(b) whose long-time diffusion constant will remain the same as that of Fig. 3(a).] But at very early time according to Eq. (10), $D(t)$ for Fig. 3(b) will be larger because it has a smaller surface-to-volume ratio. The numerical results for this simple periodic arrays of small and large squares are shown in Fig. 3(c). The lower and the upper curve show the diffusion rates for the geometries with smaller and larger squares, respectively. The inset shows the corresponding scaling plot where the time for the upper curve has been scaled by a factor of 0.25 and compared with the lower curve. As expected scaling is satisfied.

In the next section we will present results where we will show that similar scaling will hold for geometries which are of fixed porosity and obey a *dynamical scaling* in the sense alluded to in Eqs. (2) and (3). On the contrary for geometries which do not obey such scaling one observes a *crossover*. In the next section we present the detailed results.

IV. RESULTS

A. Diffusion rate in the absence of surface relaxers ($\rho=0$)

Before presenting the results let us first characterize the model Vycor and aerogel samples first. In order to study the effect of pore radius and porosity we have generated different Vycors by stopping the spinodal decomposition at $t_{\rm coarse}=100$, 500, 1000, and 2500. For a given $t_{\rm coarse,}$ different levels of etching will produce Vycors of different porosity. For example for $t_{\rm coarse}=100$, 500, and 1000, by etching up to 0.365, 0.69, and 0.775, Vycors of 80% porosities are obtained with pore diameters 7.8, 11.5, and 14 lattice units, respectively. Table I summarizes the characteristics of different Vycors.

For aerogels we have stopped the aggregation process at $t_{\rm aggre}=10$ and 200 to prepare samples of 70 and 80 % porosities. Figures 1(c) and 1(d) show snapshots of 80% porous aerogels for $t_{\rm aggre}=10$ and 200, respectively. Table II summarizes the average pore diameter and surface to volume ratios for aerogels samples.

Figures 4(a), 4(b), and 4(c) shows the effective diffusion rates $D(t)$ for model Vycors of porosities 70, 75, and 80 %, respectively. Figures 5(a) and 5(b) show the corresponding figures for aerogel. The squares and the circles represent pores with smaller and larger diameters, respectively. The pores with smaller diameters have higher S/V. Therefore at the early time, according to Eq. (10), they have a lower $D(t)$. But unlike what happens in Fig. 3, the long-time diffusion rate for the system with different pore diameters are not the same. In all the cases studied here the diffusion is characterized by a *crossover* when the diffusion for the larger diameter pores falls below that of the corresponding smaller diameter pores. Figure 6 also shows diffusion rates for 80% porous Vycor for average pore diameters 17.8 [as

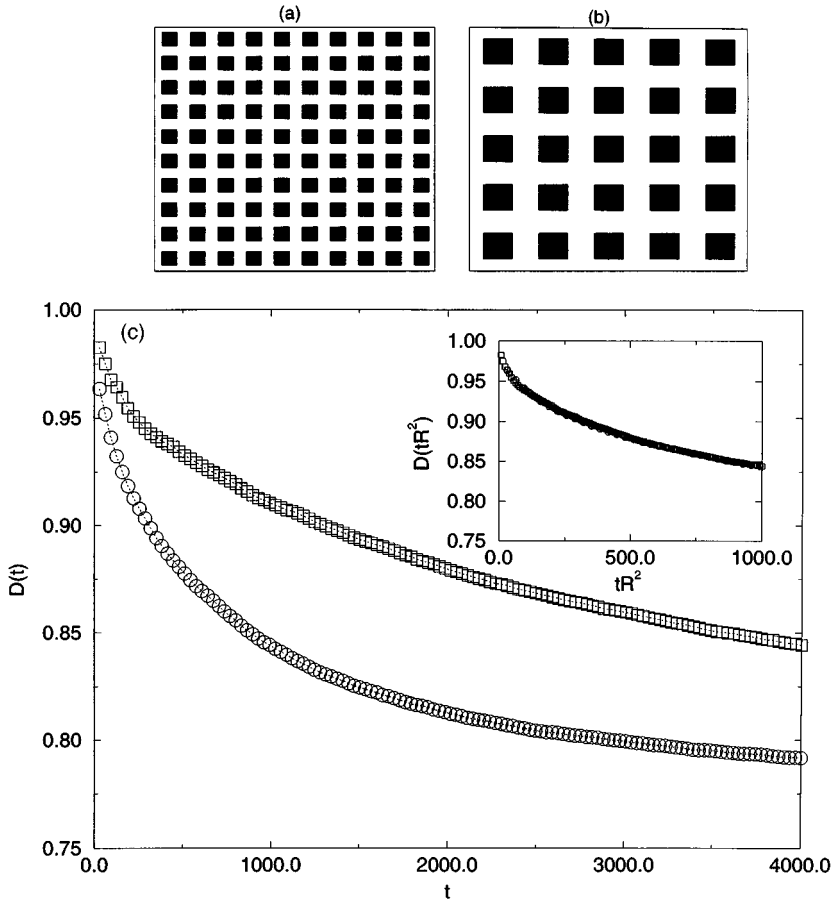

FIG. 3. Porous medium with periodic array of squares of 75% porosity. (a) Surface-to-volume ratio 0.025. (b) Surface-to-volume ratio 0.0125. (c) Diffusion rates corresponding to (a) (circles) and (b) (squares), respectively. The inset shows the corresponding scaling where the time for the upper curve has been scaled by 1/4.

shown in Fig. 4(c)] and 23.6, respectively. Unlike all the cases cited in Fig. 4, the crossover *disappears* in this figure and Fig. 6(a) resembles the case discussed in Fig. 3(c). The reason could be traced back to the scaling argument given for the square pores shown in Fig. 3. If one looks at the pictures in Figs. 1(a) and 1(b) one notices that the pores with small diameters look very different from the bigger diameter pores. Figure 1(b) cannot be obtained by a mere scaling of Fig. 1(a). In the case of the low diameter pore the pore diameter does not vary much. A random walker does not get stuck in any particular region for a long time and therefore samples the entire pore space quicker compared to what is shown in Fig. 1(b) for the large diameter pore. One notices that for the bigger diameter pores, each pore is isolated by a narrow window from the rest of the pore space. Therefore a random walker is trapped inside the pore for very long time before it gets out to make its way to a second pore where the same thing happens. Hence although at the very early time the bigger diameter pores have larger diffusion rates, eventually the effective diffusion constant for this system falls below that of the lower diameter pores. The same *crossover* is observed in aerogels as well. Hence long time diffusion constant in this class of systems *does not* depend on *porosity* only. The same argument also explains why the diffusive rate for smaller diameter pores approaches its long time value much rapidly than the larger diameter pore as seen in Fig. 4.

A critical look at the way the Vycors and aerogels are prepared can help to understand this *crossover* phenomenon better. As discussed earlier, the Vycors are prepared by a critical quench of a binary liquid mixture. Larger diameter pores are prepared by etching configurations for which

TABLE I. Porosity, average pore diameter, and surface to volume ratio for computer-generated Vycors for different ψ_{etch} and for different t_{coarse}.

t_{coarse}	ψ_{etch}	ϕ	$\langle r_{\text{pore}} \rangle$	S/V
100	0.365	0.70	7.8	0.380
500	0.690	0.70	11.5	0.263
1000	0.775	0.70	14.0	0.215
100	0.430	0.75	9.1	0.351
500	0.760	0.75	12.5	0.255
1000	0.840	0.75	15.5	0.210
100	0.490	0.80	10.8	0.314
500	0.815	0.80	14.9	0.236
1000	0.885	0.80	17.8	0.196
2500	0.945	0.80	23.6	0.192

TABLE II. Porosity, average pore diameter, and surface-to-volume ratio for computer-generated aerogels produced by DLCA method for different t_{aggre}.

t_{aggre}	ϕ	$\langle r_{\text{pore}} \rangle$	S/V
10	0.70	6.6	0.444
200	0.70	8.3	0.371
10	0.80	9.1	0.377
200	0.80	13.4	0.288

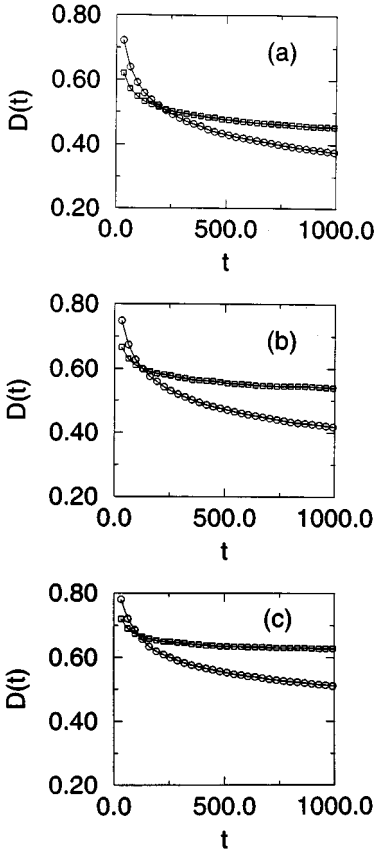

FIG. 4. (a) $D(t)$ for model Vycor with 70% porosity for average pore diameters 7.8 (squares) and 14.0 (circles), respectively. (b) $D(t)$ for model Vycor with 75% porosity for average pore diameters 9.1 (squares) and 15.5 (circles), respectively. (c) $D(t)$ for model Vycor with 80% porosity for average pore diameters 10.8 (squares) and 17.8 (circles), respectively.

t_{coarse} is large. For example a pore diameter of 7.8 is made by etching a configuration at $t_{\text{coarse}}=100$, as opposed to the case for a pore diameter of 14.0 which is prepared by etching a configuration at $t_{\text{coarse}}=1000$. It is only for the samples which are prepared from very large coarsening time (t_{coarse} large) the scaling described by Eqs. (2) and (3) holds. For the samples described in this work we have checked that the structure factors for the sample Vycors which are obtained by etching $t_{\text{coarse}}=1000$, and $t_{\text{coarse}}=2500$, respectively, exhibit dynamical scaling as described by Eqs. (2) and (3), whereas the various structure factors for the cases cited in Fig. 4 do not. The structure factors for these two samples are shown in Fig. 6(b). The inset shows the scaled structure factors where the scale factor R in each curve (at the inset) is proportional to the corresponding average pore diameter. The scaling is satisfied very well which is reflected in the scaling plots of the corresponding diffusion rates shown at the inset of Fig. 6(a). Notice that we do not have any adjustable parameter here. It is only the ratio of the pore diameters (the same as α parameter for Fig. 3) which scales both the structure factors and the corresponding diffusion constants.

Hence the scaling argument discussed in Fig. 3 breaks down for early time structures generated for the Vycors and aerogels and the asymptotic diffusion rates are different for different samples. This observation may have important application for creating environment for catalytic conversions. Depending upon the need the long-time diffusion rate could be controlled by putting samples in these model porous prepared from different coarsening regimes.

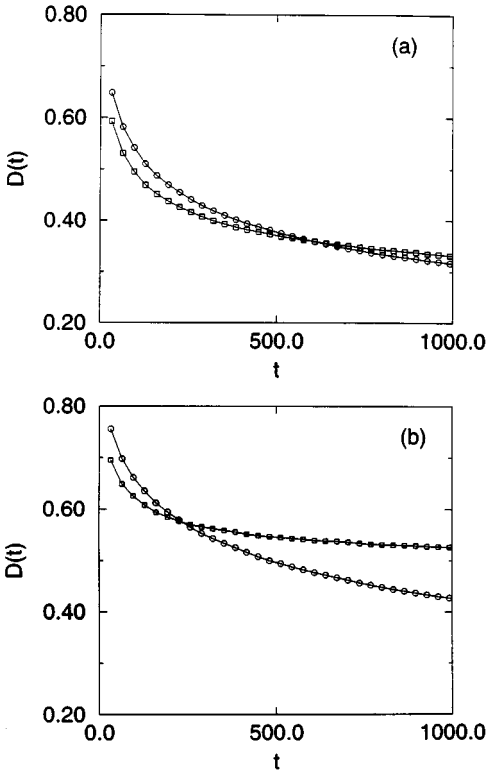

FIG. 5. (a) $D(t)$ for aerogel with 70% porosity and average pore diameters 6.6 (squares) and for 8.3 (circles), respectively. (b) $D(t)$ for aerogel with 80% porosity for average pore diameter 9.1 (squares) and for 13.4 (circles), respectively.

B. Diffusion rate in the presence of surface relaxers ($\rho \neq 0$)

Let us now consider the case when surface relaxation ρ in Eq. (1) is not equal to zero. As mentioned earlier in the introduction we model the surface relaxation with the survival probability p_f (if the random number is bigger than p_f then the walker is killed) which is connected to the parameter ρ appearing in Eq. (2). Hence $p_f=1$ will correspond to no relaxation at all while $p_f=0$ corresponds to infinite absorption.

Figures 7 and 8 show the diffusion constant $D(t)$ when the surface-relaxation strength $\gamma \neq 0$ and along with $\gamma=0$ case for comparison. Figure 7 summarizes results for the model Vycors for 70 and 80 % porosities. Figure 8 shows the corresponding figures for the aerogel. The corresponding average pore diameters and surface to volume ratios S/V could be found in Tables I and II. Since walkers get killed very rapidly in the presence of surface relaxation it has been only possible to study diffusion rates for short lengths of time until when the statistics for the surviving walkers is good. For the highest killing strength $p_f=0.4$ and the next one $p_f=0.5$ for which we carried out our diffusion studies we have taken averages over 10^6 walkers; for the rest the aver-

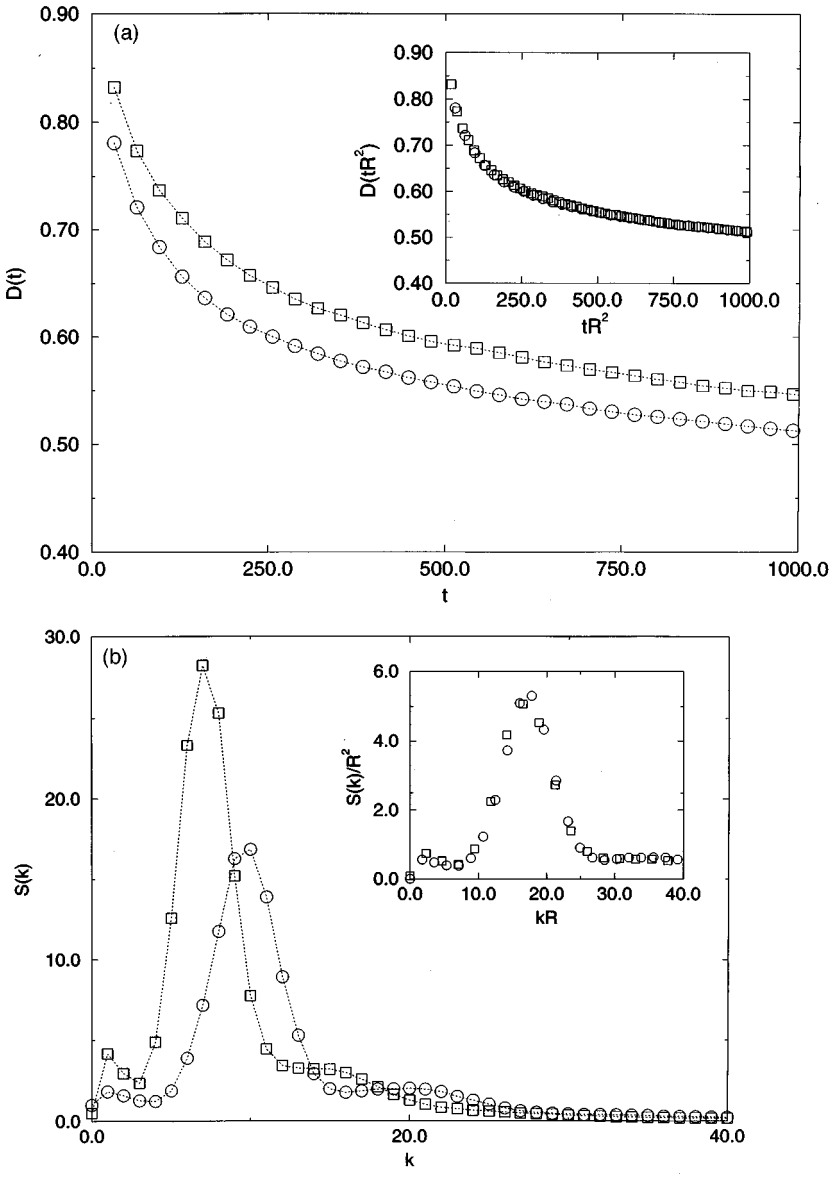

FIG. 6. (a) $D(t)$ for model Vycor with 80% porosity for average pore diameters 17.8 (circles) [as shown in Fig. 4(c)] and 23.6 (squares), respectively. The inset shows the corresponding scaling where the scale factor R for each curve is proportional to the pore diameters (1.78 and 2.36, respectively). (b) Scaling of the corresponding structure factors with the same values of R. The symbols refer to the same as in 6(a).

aging was done with 500 000 walkers. In each case we find that at early time the *presence* of the surface relaxation *enhances* the diffusion rate.

To physically understand the enhancement of the diffusion rate in the presence of surface relaxers, imagine a channel connected by dead ends as discussed by Sen *et al.*[6] (Fig. 9). The presence of these dead ends will lower the value of the diffusion constant below the value corresponding to just straight tubes. For walkers which will enter into those dead ends the $\langle r^2(t)\rangle$ will saturate very soon; therefore the overall effect will be a net decrease in the diffusion constant. Now imagine a surface relaxation is turned on at the surfaces of these dead ends but the tube is kept as it is. Those walkers which will enter into these dead ends will die very soon and will not contribute in decreasing the diffusion constant any more. Hence adding a surface relaxation in this case increases the diffusion rate. We cited this simple example to show how one can get an enhancement in diffusion rate by adding a surface relaxation term. We can think of a similar scenario taking place in our model porous media. All of them could be visualized as percolating channels with blockers. Turning on a surface relaxation will then increase the effective diffusion rate as it happens in the example given above. This is also consistent with the early time results predicted by Mitra *et al.* as described by Eq. (10). If the whole tube is now made to relax, some of the walkers will be taken away very soon before they take appreciable $\langle r^2(t)\rangle$ values and the diffusion rate will approach a smaller saturation value. The reason for the crossover that is seen in Figs. 7 and 8 is simpler than the ones shown in Figs. 4 and 5. The same surface relaxation which enhances the diffusion rate at early time also make the diffusion rate saturate faster to a smaller value as well. The crossover simply reflects the relative time of this phenomenon and the saturation values for different surface relaxation strengths. For the lower value of the surface relaxation strength, its impact at early time is less pronounced, but it is less effective too in making the diffusion rate approaching the saturation value, which is itself close to (but slightly smaller) than the saturation value in the absence of surface relaxation.

V. SUMMARY

To conclude we have presented results of random-walk simulation studies in computer-generated model 2D porous

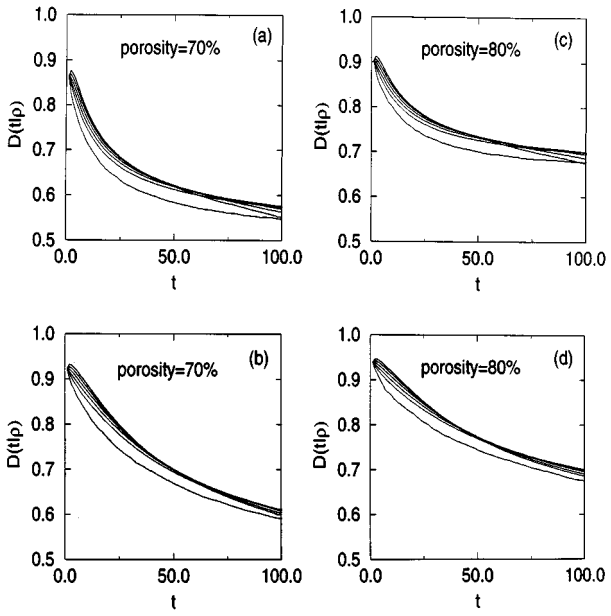

FIG. 7. $D(t|\rho)$ for Vycor with 70% and 80% porosities for different values of the survival probability p_f (0.4, 0.5, 0.6, 0.7, 0.8, and 1.0 counted from the top to the bottom from the upper left corner). $p_f=1$ corresponds to no relaxation at the surface. (a) and (b) correspond to 70% porosity and for average pore diameters 7.8 and 14.0, respectively. (c) and (d) correspond to 80% porosity and for average pore diameters 10.8 and 17.8, respectively.

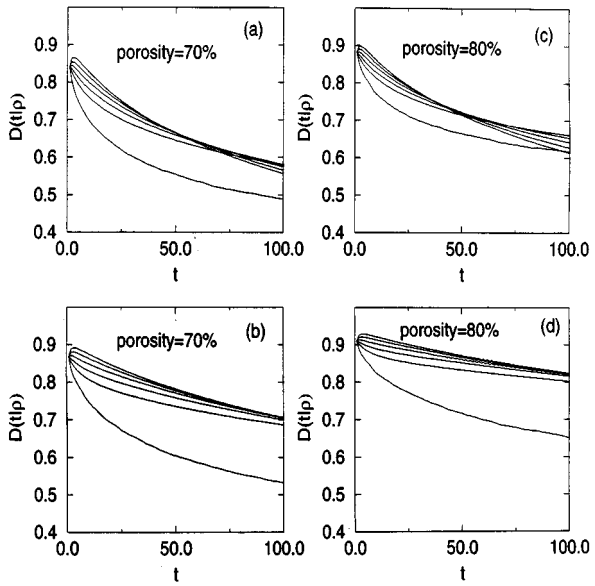

FIG. 8. $D(t|p)$ for aerogel with 70% and 80% porosities for different values of the survival probability p_f (0.4, 0.5, 0.6, 0.7, 0.8, and 1.0 counted from the top to the bottom from the upper left corner). $p_f=1$ corresponds to no relaxation at the surface. (a) and (b) correspond to 70% porosity and for average pore diameters 6.6 and 8.3, respectively. (c) and (d) correspond to 80% porosity and for average pore diameters 9.1 and 13.4, respectively.

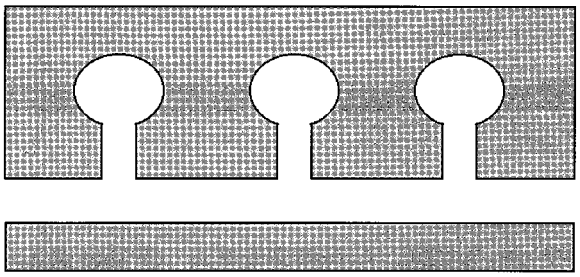

FIG. 9. Picture of a tube connected to dead ends.

media of relatively high porosity. In particular the two types of porous media considered here resemble Vycors and aerogels. These porous media have drawn considerable attention in recent years due to the fact that physical systems exhibit very different behavior when imbibed into these materials. We have calculated the structure factor for these materials. When diffusion rate is compared for different samples of fixed porosity, if the structure factors of any two samples do not exhibit *dynamical scaling* (in the same way various late time configurations of a binary liquid mixture do), the diffusion rates will exhibit a *crossover*. This is true for a set of model Vycors and aerogels samples. To establish this fact we have shown a counter example where two different Vycor samples, both of them prepared from late time (t_{coarse} large) configurations do not exhibit crossover. The snapshots of different samples help to understand this phenomenon better. In both Vycors and in aerogels the surfaces of larger diameter samples form a more correlated pattern; our computer generated pictures show that the pore geometries akin to large pore spaces separated by *narrow but correlated walls*, and having *narrow throats*. Therefore although the pore radii are larger the long time diffusion rate becomes smaller. It also takes longer time to reach its saturation value. Surface relaxation enhances the diffusion rate at early time. We draw an analogy with a much simpler geometry of tube with dead ends proposed by Sen *et al.* A crossover in diffusion rate, *albeit* of different origin, is also observed for a given geometry for different surface relaxation strengths. We also find that for smaller pores the magnetic relaxation is characterized by a single relaxation time which decreases with the enhanced strength of the uniform surface relaxers. The bigger pores however show an initial nonexponential decay followed by an exponential decay. It would be interesting to study the effect of nonuniform surface relaxivity which we plan to report in a future publication We are planning to extend our calculations for a real 3D Vycor and to incorporate pulsed field gradient NMR into this scheme.

ACKNOWLEDGMENTS

This work has been supported by NSF Grants No. CHE-92 24102 (A.B. and S.D.M.) and DMR-9312596 (A.C.). We thank J. R. Banavar for many useful discussions.

[1] J. R. Banavar and L. M. Schwartz, in *Molecular Dynamics in Restricted Geometries*, edited by J. Klafter and J. M. Drake (Wiley, New York, 1989), p. 273.
[2] K. R. Brownstein and C. E. Tarr, Phys. Rev. A **19**, 2446 (1979).
[3] J. R. Banavar and L. M. Schwartz, Phys. Rev. Lett. **58**, 1411 (1987).
[4] L. M. Schwartz and J. R. Banavar, Phys. Rev. B **39**, 11 965 (1989).
[5] P. N. Sen, L. M. Schwartz, P. P. Mitra, and P. LeDoussal, Phys. Rev. Lett. **65**, 3555 (1992).
[6] P. N. Sen, L. M. Schwartz, P. P. Mitra, and B. Halperin, Phys. Rev. B **49**, 215 (1994).
[7] P. P. Mitra and P. N. Sen, Phys. Rev. B **45**, 143 (1992).
[8] P. P. Mitra and P. N. Sen, Phys. Rev. B **47**, 8565 (1993).
[9] D. J. Bergman and K.-J. Dunn, Phys. Rev. B **51**, 3401 (1995).
[10] D. J. Bergman, K.-J. Dunn, L. M. Schwartz, and P. P. Mitra, Phys. Rev. B **51**, 3393 (1995).
[11] See, for example, W. I. Goldburg in *Dynamics of Ordering Processes in Condensed Matter*, edited by S. Komura and H. Furukawa (Plenum, New York, 1988) and W. I. Goldburg, F. Aliev, and X. L. Wu, Physica A **213**, 61 (1995), and references therein.
[12] For a detailed discussion of the structure of Vycor glass and a three-dimensional computer modeling see, L. Monette, G. S. Grest, and M. P. Anderson, Phys. Rev. E **50**, 3361 (1994).
[13] For a review, see J. D. Gunton, M. San Miguel, and P. S. Sahni, in *Phase Transition and Critical Phenomena*, edited by C. Domb and J. L. Lebowitz (Academic, London, 1983), Vol. 8. See also, Ref. 14.
[14] A. J. Bray, Adv. Phys. **43**, 357 (1994), for a more recent review.
[15] J. D. Gunton, E. T. Gawlinski, A. Chakrabarti, and K. Kaski, J. Appl. Crystallogr. **21**, 811 (1988).
[16] Y. Oono and S. Puri, Phys. Rev. Lett. **58**, 863 (1987).
[17] A. Chakrabarti, Phys. Rev. Lett. **69**, 1548 (1992).
[18] R. Jullien and R. Botet, *Aggregation and Fractal Aggregates* (World Scientific, Singapore, 1987).
[19] A. Hasmy, E. Anglaret, M. Foret, J. Pelous, and R. Jullien, Phys. Rev. B **50**, 6006 (1994); K. Uzelac, A. Hasmy, and R. Jullien, Phys. Rev. Lett. **74**, 422 (1995).
[20] T. Sintes, R. Toral, and A. Chakrabarti, Phys. Rev. E **50**, R3330 (1994).
[21] K. S. Mendelson, Phys. Rev. B **47**, 1081 (1993); **41**, 562 (1990).
[22] M. Lipsicas, J. R. Banavar, and J. Willemsen, Appl. Phys. Lett. **48**, 1544 (1986).
[23] M. H. Cohen and K. Mendelson, J. Appl. Phys. **53**, 1127 (1982).
[24] J. W. Haus and K. W. Kher, Phys. Rep. **150**, 263 (1987).